the $d\sigma^*$ orbital, because these should be red-shifted significantly in d^8–d^8 Pt_2 species. The $d\sigma^* \rightarrow d_{x^2-y^2}$ excitations, $^1A_{1g} \rightarrow {}^{1,3}B_{2u}$ and $^{1,3}B_{1g}$, include just one dipole-allowed transition, that to $E_u(^3B_{2u})$.

We suggest that the 313-nm band involves excitation to $E_u(^3B_{2u})$, as, taking account of the influence of absorption due to surrounding bands, it appears to be about twice as intense in σ as in π polarization, which is consistent with an x,y-dipole-allowed transition. Moreover, Isci and Mason's MCD data[1e] are consistent with a negative A term for this band in aqueous solution. (The interpretation of the data by Isci and Mason was different, but needs to be modified because of our other results.)

The 286-nm band appears to be just slightly more intense in π polarization than in σ. This is not consistent with either molecular z or x,y polarization. The MCD data show only a B term[1e] coincident with the absorption maximum. The mixed polarization behavior suggests that the intensity may be vibronically induced and that the band may represent an orbitally forbidden transition to one or more of the singlet d–d states. In Table I we assign the band to $^1A_{1g} \rightarrow {}^1B_{2u}$, as the inferred $^{1,3}B_{2u}$ splitting is reasonable for a d–d transition.[16]

Comparison to Other Work. Isci and Mason have presented MCD data for $Pt_2(P_2O_5H_2)_4^{4-}$ in aqueous solution.[1e] Our results are generally compatible with theirs; in particular, they found a distinct A term for the ~250-nm band, consistent with our assignment to $^1A_{1g} \rightarrow E_u(^3E_u)$. Comparison to the spectra of d^8–d^8 Rh_2 compounds indicates[10] that the ~250-nm band is far weaker than expected for the singlet–singlet transition. With this change, all of Isci and Mason's assignments other than those for the $^{1,3}A_{2u}(d\sigma^* \rightarrow p\sigma)$ states need to be modified.

Our assignments (Figure 7 and Table I) also differ in detail from those proposed by Shimizu et al.,[2] which were based on fits to spin–orbit calculations. However, the energies of the $^{1,3}E_u(d_{xz},d_{yz} \rightarrow p\sigma)$ states are close to their predictions; as these states are the ones that determine the $A_{1u},E_u(^3A_{2u})(d\sigma^* \rightarrow p\sigma)$ spin–orbit splitting, the calculation of this splitting is reasonable.[2]

An interesting point is that we have been able to locate d–d excited states for $Pt_2(P_2O_5H_2)_4^{4-}$: states of this type have been postulated[17] to be important in thermally activated nonradiative decay of Rh(I) binuclear compounds. Our results provide a benchmark example that will aid in the estimation of the energies of d–d states in other d^8–d^8 species. For $Pt_2(P_2O_5H_2)_4^{4-}$ itself, the d–d states are clearly much too energetic to be accessible thermally from the emissive $^{1,3}A_{2u}$ states.

Acknowledgment. Assistance from the staff of the Center for Fast Kinetics Research (supported jointly by the Biotechnology Branch of the Division of Research Resources of NIH (Grant RR00886) and The University of Texas at Austin) is gratefully acknowledged. This research was supported by National Science Foundation Grant CHE84-19828 and the Caltech President's Fund.

Registry No. $(n\text{-}Bu_4N)_4[Pt_2(P_2O_5H_2)_4]$, 89462-52-2.

(15) Cowman, C. D.; Gray, H. B. *Inorg. Chem.* **1976**, *15*, 2823–2824.
(16) Tuszynski, W.; Gliemann, G. *Z. Naturforsch., A: Phys., Phys. Chem., Kosmophys.* **1979**, *34A*, 211–219.
(17) Rice, S. F.; Milder, S. J.; Gray, H. B.; Goldbeck, R. A.; Kliger, D. S. *Coord. Chem. Rev.* **1982**, *43*, 349–354.

Contribution from the Department of Chemistry, The University of North Carolina, Chapel Hill, North Carolina 27514, and Laboratory of Chemical Biodynamics, Lawrence Berkeley Laboratory, University of California, Berkeley, California 94720

Intramolecular Electron Transfer in the Reductive Chromophore–Quencher Complex $[(bpy)Re(CO)_3(py\text{-}PTZ)]^+$

Pingyun Chen,[†] T. David Westmoreland,[†] Earl Danielson,[†] Kirk S. Schanze,[‡] Doug Anthon,[‡] Paul E. Neveux, Jr.,[†] and Thomas J. Meyer*[†]

Received June 16, 1986

Three metal complexes containing the reductive quencher ligand py-PTZ, $[(bpy)Re(CO)_3(py\text{-}PTZ)]^+$ and $[(bpy)_2Ru^{II}L(py\text{-}PTZ)]^{n+}$ (where $L = Cl^-$ ($n = 1$) and acetonitrile ($n = 2$)), were prepared and their redox and spectral properties investigated. The chromophore–quencher complexes have essentially the same photophysical properties as their corresponding pyridine analogues at 77 K in a 4:1 (v/v) ethanol/methanol glass, but their properties are profoundly different in fluid solution. For the Re complex in fluid solution excitation of the $Re \rightarrow \pi^*(bpy)$ metal to ligand charge-transfer (MLCT) chromophore at 355 nm is followed by rapid (<10 ns) appearance of transient absorption (TA) features at 350 and 500 nm consistent with formation of the charge-separated state $[(bpy^{\bullet-})Re(CO)_3(py\text{-}PTZ^{\bullet+})]^{+*}$. Picosecond TA experiments monitored at 500 nm show that the $PTZ^{\bullet+}$ site grows in within ~200 ps in polar organic solvents following laser excitation at 355 nm. The transient behavior observed leads to the conclusion that initial excitation of the MLCT chromophore is followed by rapid intramolecular electron-transfer quenching with $k_q(RT) = 4.8 \times 10^9\ s^{-1}$ in acetonitrile to give the charge-separated excited state $[(bpy^{\bullet-})Re(CO)_3(py\text{-}PTZ^{\bullet+})]^+$, which, in turn, decays to the ground state with $k_2 = 4.0 \times 10^7\ s^{-1}$.

Introduction

Oxidative- and reductive-electron-transfer quenching of the metal to ligand charge-transfer (MLCT) excited states of $Ru(bpy)_3^{2+}$ (bpy is 2,2′-bipyridine) and related complexes are well-defined processes, e.g., eq 1[1] (PQ^{2+} is N,N'-dimethyl-

$$\begin{aligned} Ru(bpy)_3^{2+} + h\nu &\rightarrow Ru(bpy)_3^{2+*} \\ Ru(bpy)_3^{2+*} + PQ^{2+} &\rightarrow Ru(bpy)_3^{3+} + PQ^{\bullet+} \\ Ru(bpy)_3^{2+*} + PTZ &\rightarrow Ru(bpy)_3^{+} + PTZ^{\bullet+} \end{aligned} \qquad (1)$$

4,4′-bipyridinium ion; PTZ is phenothiazine). A detailed understanding of the electron-transfer events that occur during and after the quenching step is restricted by the absence of structural information, which is an inherent limitation given the outer-sphere nature of the electron-transfer reactions involved.[1e,2] In part to

(1) (a) Meyer, T. J. *Acc. Chem. Res.* **1978**, *11*, 94. (b) Kalyanasundaran, K. *Coord. Chem. Rev.* **1982**, *46*, 159. (c) Al-Saigh, H. Y.; Kemp, T. J. *J. Chem. Res., Miniprint* **1984**, 2001. (d) Whitten, D. G. *Acc. Chem. Res.* **1980**, *13*, 83. (e) Sutin, N.; Creutz, C. *Pure Appl. Chem.* **1980**, *52*, 2717. (f) Balzani, V.; Bolletta, F.; Gandolfi, M. T.; Maestri, M. *Top. Curr. Chem.* **1978**, *75*, 1.
(2) (a) Meyer, T. J. *Prog. Inorg. Chem.* **1983**, *30*, 389. (b) Newton, M. D.; Sutin, N. *Annu. Rev. Phys. Chem.* **1984**, *35*, 437. (c) Isied, S. S. *Prog. Inorg. Chem.* **1984**, *32*, 443. (d) Haim, A. *Prog. Inorg. Chem.* **1983**, *30*, 273. (e) Balzani, V.; Scandola, F. In *Energy Resources Through Photochemistry and Catalysis*; Grätzel, M., Ed.; Academic: New York, 1983; Chapter 1.

[†] The University of North Carolina.
[‡] University of California.

0020-1669/87/1326-1116$01.50/0

overcome such limitations, a series of studies have appeared based on optically induced intramolecular electron transfer in ligand-bridged dimers[3] and mixed-valence complexes[3,4] and in chromophore–quencher (CQ) complexes where a chemical link exists between the chromophore to be excited and a potential electron-transfer donor or acceptor. Among such systems are several examples of quinones attached to porphyrins[5] and from our own work examples where MLCT excitation is followed by intramolecular electron transfer,[6] e.g.

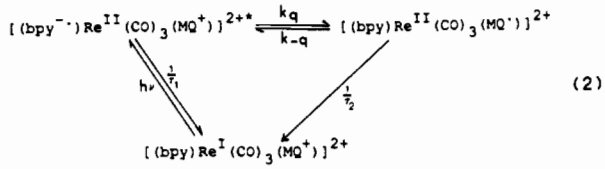

(2)

(MQ^+ is *N*-methyl-4,4′-bipyridinium ion)

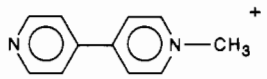

MLCT excited states can undergo either oxidative or reductive quenching, and we report here on the preparation and properties of three complexes that contain both an MLCT chromophore and the chemically attached reductive quencher ligand, 10-(4-picolyl)phenothiazine (py-PTZ). For the complex $[(bpy)Re(CO)_3(py\text{-}PTZ)]^+$, there is clear evidence that MLCT excitation is followed by intramolecular reductive quenching and the processes observed are illustrative in interrelating a number of phenomena observed in related systems. Part of this work has appeared in a preliminary communication.[7]

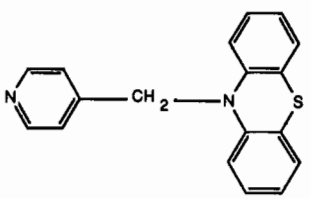

py-PTZ

Experimental Section

A. Materials. All solvents for preparative experiments were reagent grade; solvents for electrochemical and spectroscopic experiments were spectroquality (Burdick and Jackson). The 4:1 (by volume) EtOH/MeOH mixture used for temperature-dependent studies of luminescent lifetimes and emission spectra was prepared from spectroquality solvents, which were dried by distillation from Mg/I_2 and subsequent drying over activated powdered (EtOH) or bead (MeOH) molecular sieves. Supporting electrolyte for all electrochemical measurements was tetraethylammonium hexafluorophosphate (TEAH), which was recrystallized prior to use.

B. Preparations. 10-(4-Picolyl)phenothiazine (py-PTZ). The donor quencher ligand was prepared by reacting the lithio salt of phenothiazine (PTZ) anion generated in situ with 4-(chloromethyl)pyridine in dry THF solution. Lithium diisopropyl amide (LDA) was generated by mixing 3 mL of freshly distilled diisopropyl amine in 5 mL of THF with 13.5 mL of a 1.6 M solution of butyllithium in hexane. This solution was added dropwise to 4 g of PTZ dissolved in 20 mL of THF. After 15 min, the solution had assumed the orange color of the PTZ anion. The reaction mixture was immersed in an ice bath as 1.35 g of solid 4-(chloromethyl)pyridine hydrochloride were added. The solution developed a red color within a few minutes. The mixture was stirred and allowed to warm up slowly to room temperature overnight. The solvent was removed from the red-brown suspension and the product purified by flash chromatography on a neutral silica gel column using 49:31:20 hexane/toluene/ethyl acetate as eluant. Anal. Calcd: C, 74.45; H, 4.83; N, 9.65; S, 11.06. Found: C, 73.85; H, 4.57; N, 9.51; S, 10.84. The proton NMR spectrum of py-PTZ in $CDCl_3$ solution (vs. Me_4Si) has the following general features: δ 8.54 (doublet of doublets; area 2), 7.02 (overlapping multiplets; area 8), 6.54 (doublet of doublets; area 2), 5.03 (singlet; area 2).

***fac*-[(bpy)Re(CO)$_3$(py-PTZ)](PF$_6$).** The chromophore quencher complex was prepared by a reaction between the trifluoromethanesulfonato derivative of the Re complex[8] and an excess of the py-PTZ ligand. A 0.401-g (0.696-mmol) sample of $[(bpy)Re(CO)_3(TFMS)]$ (TFMS is trifluoromethanesulfonate) was heated at reflux in 2:1 EtOH/water with 0.35 g (1.21 mmol, 1.7 equiv) of py-PTZ for 2 h. The solution was allowed to cool, and a precipitate formed. The solid was redissolved by adding a small amount of acetone. An excess of a saturated solution of NH_4PF_6 was added and the solvent mixture removed by rotary evaporation. The residue was dissolved in CH_2Cl_2 and added to isooctane. The precipitate was collected and reprecipitated once more. The light yellow product[9] was obtained in 68% yield based on Re. Anal. Calcd: C, 43.19; H, 2.55; N, 6.5; S, 3.73. Found: C, 44.26; H, 2.59; N, 6.41; S, 4.41. The ^1H NMR spectrum in CD_3CN solution (vs. Me_4Si) showed the following features: δ 9.17 (doublet; area 2), 8.34 (doublet; area 2), 8.24 (triplet; area 2), 8.10 (doublet; area 2), 7.75 (triplet; area 2), 7.34 (doublet, area 2), 7.11 (doublet; area 2), 6.85–7.05 (overlapping triplets; area 4), 6.55 (doublet; area 2), 5.05 (singlet; area 2).

***fac*-[(bpy)Re(CO)$_3$(4-Etpy)](PF$_6$).** The model, 4-ethylpyridine (4-Etpy) complex was prepared by a literature procedure.[10]

[(bpy)$_2$RuCl(py-PTZ)](PF$_6$). The Ru complex was prepared by displacement of Cl^- from the *cis*-dichloro complex[11] by excess py-PTZ in EtOH/water. A 26-mg (0.05-mmol) sample of $(bpy)_2RuCl_2\cdot 2H_2O$ and 36 mg (0.124 mmol, 2.48 equiv) of py-PTZ were added to a 1:1 EtOH/water solution and the mixture heated at reflux for 3 h. The reaction mixture was allowed to cool to room temperature. An excess of NH_4PF_6 was added to the reaction mixture via a saturated aqueous solution, and a brown precipitate formed. The precipitate was filtered and washed with water. The crude product was purified by reprecipitation from acetonitrile upon addition of ether. Anal. Calcd: C, 51.6; H, 3.40; N, 9.51; S, 3.63. Found: C, 50.49; H, 3.53; N, 9.18; S, 4.04.

[(bpy)$_2$Ru(CH$_3$CN)(py-PTZ)](PF$_6$)$_2$. The acetonitrile complex was prepared in a stepwise manner via the analogous aquo complex, $[(bpy)_2Ru(H_2O)_2]^{2+}$, by mixing 48 mg (0.10 mmol) of $(bpy)_2Ru(CO_3)$ and 25 μL (2 equiv) of CF_3COOH in water. The resulting solution was stirred for 10 min followed by addition of 84 mg (0.29 mmol, 2.9 eq.) of py-PTZ. The mixture was heated at reflux for 3 h. NH_4PF_6 in excess was added to the reaction mixture as a saturated aqueous solution. The solution was allowed to cool, and a precipitate was collected. The precipitate was dissolved in acetonitrile, at which point exchange of H_2O by CH_3CN occurs, and was chromatographed on an alumina column with 1:1 toluene/acetonitrile as eluant. Anal. Calcd: C, 46.41; H, 3.19; N, 9.48. Found: C, 46.23; H, 3.22; N, 8.94.

C. Measurements. Cyclic voltammetry (CV) and coulometric experiments were carried out by using a PAR Model 173 potentiostat. The

(3) (a) Creutz, C.; Kroger, P.; Matsubara, T.; Netzel, T. L.; Sutin, N. *J. Am. Chem. Soc.* **1979**, *101*, 5442. (b) Schanze, K. S.; Meyer, T. J. *Inorg. Chem.* **1985**, *24*, 2121. Schanze, K. S.; Neyhart, G. A.; Meyer, T. J. *J. Phys. Chem.* **1986**, *90*, 2182. (c) Curtis, J. C.; Bernstein, J. S.; Schmehl, R. H.; Meyer, T. J. *Chem. Phys. Lett.* **1981**, *81*, 48. Curtis, J. C.; Bernstein, J. S.; Meyer, T. J. *Inorg. Chem.* **1985**, *24*, 385.

(4) (a) Creutz, C. *Prog. Inorg. Chem.* **1983**, *30*, 1. (b) Taube, H. In *Tunneling in Biological Systems*; Chance, B., et al., Eds.; Academic: New York, 1979; p 173. (c) Richardson, D. E.; Taube, H. *J. Am. Chem. Soc.* **1983**, *105*, 40. (d) Meyer, T. J. In *Mixed-Valence Compounds*; Brown, D. B., Ed.; D. Reidel: Dordrecht, The Netherlands, 1979; p 75.

(5) (a) Ho, T.; McIntosh, A. R.; Bolton, J. R. *Nature (London)* **1980**, *286*, 254. (b) Nishitani, S.; Kurata, N.; Sakata, Y.; Misuni, S. *Tetrahedron Lett.* **1981**, *22*, 2099. (c) Bergkamp, M. A.; Dalton, J.; Netzel, T. L. *J. Am. Chem. Soc.* **1982**, *104*, 253. (d) Joran, A.; Leland, B.; Geller, G.; Hopfield, J. J.; Dervan, P. B. *J. Am. Chem. Soc.* **1984**, *106*, 6090. (e) McIntosh, A. R.; Siemiarczuk, A.; Bolton, J. R.; Stillman, M. J.; Roach, K. J.; Weedon, A. C. *J. Am. Chem. Soc.* **1983**, *105*, 7215. (f) Siemiarczuk, A.; McIntosh, A. R.; Ho, T.-F.; Stillman, M. J.; Roach, K. J.; Weedon, A. C.; Bolton, J. R.; Connolly, J. S. *J. Am. Chem. Soc.* **1983**, *105*, 7224. (g) Schmidt, J. A.; Siemiarczuk, A.; Weedon, A. C.; Bolton, J. R. *J. Am. Chem. Soc.* **1985**, *107*, 6112. (h) Gust, D.; Moore, T. A. *J. Photochem.* **1985**, *29*, 173.

(6) (a) Sullivan, B. P.; Abruna, H. D.; Finklea, H. O.; Salmon, D. J.; Nagle, J. K.; Meyer, T. J.; Sprintrchnik, H. *Chem. Phys. Lett.* **1978**, *58*, 389. (b) Westmoreland, T. D.; LeBozec, H.; Murray, R. W.; Meyer, T. J. *J. Am. Chem. Soc.* **1983**, *105*, 5952.

(7) Westmoreland, T. D.; Schanze, K. S.; Neveux, P. E.; Danielson, E.; Sullivan, B. P.; Chen, P. Y.; Meyer, T. J. *Inorg. Chem.* **1985**, *24*, 2596.

(8) Sullivan, B. P.; Meyer, T. J. *J. Chem. Soc., Chem. Commun.* **1984**, 1244.

(9) The complex was purified further by chromatography on a silica gel column using 35% acetonitrile in toluene as eluant. However, there was no noticeable change in either the lifetime or emission properties of the purified sample.

(10) Caspar, J. V.; Meyer, T. J. *J. Phys. Chem.* **1983**, *87*, 952.

(11) Sullivan, B. P.; Salmon, D. J.; Meyer, T. J. *Inorg. Chem.* **1978**, *17*, 3335.

Table I. Spectral and Electrochemical Data in Acetonitrile

complexes	λ_{max},[a] nm (ϵ, M^{-1} cm^{-1})		λ_{em},[b] nm	$E_{1/2}$,[c] V vs. SSCE		
	$\pi\pi^*$	MLCT		Ru(III/II) or Re(II/I)	$PTZ^{+/0}$	$bpy^{0/-}$
$[(bpy)Re(CO)_3(4\text{-}Etpy)]^+$	308 (1.2×10^4) 320 (1.3×10^4)	350 (4.0×10^3)	505	1.72[d]		−1.18[d]
$[(bpy)Re(CO)_3(py\text{-}PTZ)]^+$	308 (1.7×10^4) 320 (1.7×10^4)	350 (4.5×10^3)[e]	505	1.60[f]	0.83	−1.13
$[(bpy)_2RuCl(py\text{-}PTZ)]^+$	294 (5.2×10^4)	356 (1.3×10^4) 500 (9.2×10^3)	669 731	0.83[g]	0.83[g]	−1.48
$[(bpy)_2Ru(CH_3CN)(py\text{-}PTZ)]^{2+}$	288 (4.3×10^4)	436 (7.5×10^3)	567 610	1.39	0.83	−1.34 −1.56

[a] The number in parenthese is the molar extinction coefficient for the wavelength cited in acetonitrile. There are two distinct bands in the visible region for $[(bpy)_2RuCl(py\text{-}PTZ)]^+$, which were also observed in its pyridine analogue, see ref 16. [b] Emission spectra for Ru complexes were taken at 77 K in 4:1 (v/v) EtOH/MeOH in a finger Dewar excited at the maxima of the lowest energy absorption bands. Emission spectra for the Re complexes were obtained in an Oxford Instrument cryostat at 80 K excited at 385 nm. Vibrational structure was observed in the spectra of the Ru complexes, the components of which were separated by approximately 1300 cm^{-1}. [c] All $E_{1/2}$ values were obtained from the average of the potentials of the cathodic and anodic current peaks in cyclic voltammograms in acetonitrile solution with tetraethylammonium hexafluorophosphate as the supporting electrolyte. [d] Data were taken from ref 10. [e] A broad shoulder centered approximately at 350 nm; the extinction coefficient was calculated from the absorbance at the wavelength given. [f] Chemically irreversible; the potential cited is the peak potential. [g] A broad; two-electron oxidation wave, see Results on electrochemistry for details.

CV experiments were conducted with Pt-bead working, Pt-wire auxiliary and saturated sodium calomel (SSCE) reference electrodes in a one-compartment cell. Samples were dissolved in spectroquality acetonitrile with approximately 0.1 M TEAH as the supporting electrolyte and deoxygenated by N_2 bubbling for at least 5 min prior to a scan. All potentials are reported vs. SSCE and are uncorrected for junction potentials. Coulometric experiments were carried out in a three-compartment cell under a dry N_2 atmosphere by using a platinum-mesh working electrode. The absorption spectra were obtained from the solution in the working compartment only.

UV–visible spectra were recorded on HP 8450A and HP8451A diode array spectrometers. Emission spectra were obtained on an SLM Instrument Model 8000 photon-counting fluorometer. Spectra were corrected for detector sensitivity by using the data and the program supplied with the instrument. Corrected excitation spectra were obtained by using the same instrument in a ratio recording mode with Rhodamine B dissolved in ethylene glycol (5×10^{-3} M) in a triangular cell as a quantum counter. Temperature-dependent experiments were conducted on an Oxford Instruments DN1704 Cryostat and temperature controller. Samples were cooled down from high temperature to lower temperature and equilibrated for at least 15 min at each temperature in lifetime measurements and equilibrated for 30 min in emission-intensity measurements. The emission spectra at 77 K were obtained with the use of a finger Dewar. The conventional flash photolysis experiments were conducted by using a system that has been reported in detail previously.[12]

Luminescence lifetimes were obtained by monitoring the emission decay subsequent to 337-nm pulse excitation (10 ns fwhm, 0.5 mJ) with a Molectron UV-400 N_2 laser. Emission was monitored at a right angle to the excitation beam with a Bausch & Lomb Model 33-86-02 grating monochromator and a HAMAMATSU R928 photomultiplier in an EMI Gencom RFI/S housing. Additional filtering was provided by nitromethane contained in a cell fitted in the front of the entrance slit of the monochromator to absorb the scattered light from the laser. The photomultiplier signal was an output to a Tektronix Model 7912 AD Transient Digitizer and then into a PDP 11/34 minicomputer. The lifetimes were determined by a weighted least-squares procedure fit to a single exponential decay.

Transient absorbance (TA) signals were acquired following pulse excitation at 355 nm by a Quanta-Ray DCR 2A Nd:YAG laser (third harmonic, 10-ns fwhm, 10 mJ/pulse) with an OSRAM XBO 150-W Xe lamp as the monitoring light. The lamp was housed in a Photochemical Research Associates (PRA) ALH 215 housing and powered by a PRA Model 301 power supply externally modulated. A shutter placed between the monitoring lamp and the cell was opened for 5-ms intervals to prevent PMT fatigue and sample photolysis. The monitoring light was focused at the cell, collimated after the cell, and finally focused onto the entrance slit of a Bausch and Lomb 0.50-m grating monochromator (f 3.5). Transient signals were detected by a five-stage (RCA 4840) PMT housed at the exit slit of the monochromator. The output from the PMT was terminated into a 50-Ω resistor and recorded by a Tektronix 7912 AD transient digitizer interfaced to a PDP 11/34 computer. The TA spectra were plotted as $\Delta A = \log (I_0/I_t)$ vs. monochromator wavelength where I_0 was the monitoring light intensity prior to laser pulse and I_t the observed signal at delay time t. The transient lifetimes were obtained by analyzing the transient decay curve as described above.

The picosecond time-resolved transient absorption measurements were conducted by using a streak camera detection technique described recently.[13] A brief summary follows. A signal pulse from the pulse train of an actively and passively mode locked Nd:YAG laser was amplified and passed through a KDP crystal to generate the third harmonic (355 nm, ~1.0 mJ). The third harmonic was split with a beam splitter with ~50% of the power being used to excite a strongly fluorescing "probe" solution[14] and ~50% delayed temporally and then used to excite the sample. By the use of a series of mirrors and lenses, the probe fluorescence and the pump beam were made collinear and focused onto a small aperture at the sample cell. After the cell the pump beam was diverted into a beam stop and the probe fluorescence was imaged onto a computer-controlled streak camera detector system. Data acquisition required first the accumulation of a series of streak traces with the pump beam blocked (I_0) and then a series of traces with the pump beam unblocked ($I_0 + \Delta I$); generally 1000 pulses were averaged. The transient absorption traces were reconstructed by computer subtraction of the accumulated data.[15] The detection wavelength was chosen by placing interference filters into the path of the probe fluorescence before it impinged onto the sample cells. Samples were contained in 1 × 1 cm cells and had optical densities >2.0 at the excitation wavelength. The sample was stirred vigorously during data acquisition.

In the traces clear evidence was obtained for the appearance of $PTZ^{\bullet+}$ by a prompt process, which occurred during the laser pulse, and a slower process, which was time resolved. The temporal absorption characteristics of the slower process were calculated by

$$\Delta A(t) = \alpha_{slow} \exp(t/\tau_{slow}) + \alpha_{prompt} A_{prompt} \quad (3)$$

where α_{slow} and α_{prompt} are the fractions of $PTZ^{\bullet+}$ produced by the two processes and $\alpha_{prompt} A_{prompt}$ is the component of the absorption change that occurs during the laser pulse.

Samples for temperature-dependent studies of luminescent lifetimes and emission spectra were prepared in a drybox. Samples for TA experiments were degassed by N_2 bubbling for 20 min. The emission intensities used in calculating normalized relative emission intensities are taken as the height of the emission maximum at a given temperature. Corrections for bandwidth, absorbance of the sample, transparency of the glass, and other temperature-dependent factors were not taken into account.

Results

UV–Visible Absorption Spectra. Absorption bands and molar extinction coefficients for the three complexes in acetonitrile solution are summarized in Table I. The lowest energy bands

(12) Young, R. C.; Keene, F. R.; Meyer, T. J. *J. Am. Chem. Soc.* **1977**, *99*, 2468.

(13) (a) Anthon, D. Ph.D. Dissertation, University of California at Berkeley, 1986. (b) Yeh, S. W. Ph.D. Dissertation, University of California at Berkeley, 1985.

(14) The "probe" fluorescence solution consisted of a concentrated methanol solution of a long-lived sensitizer (9,9′-bianthryl) and a dye that was strongly fluorescent at the wavelength of interest (coumarin 500).

(15) In order to generate $\Delta A(t)$ plots a computer routine carried out the following computation: $\Delta A(t) = \ln [I(t)_{no\ excitation}] - \ln [I(t)_{excited}]$.

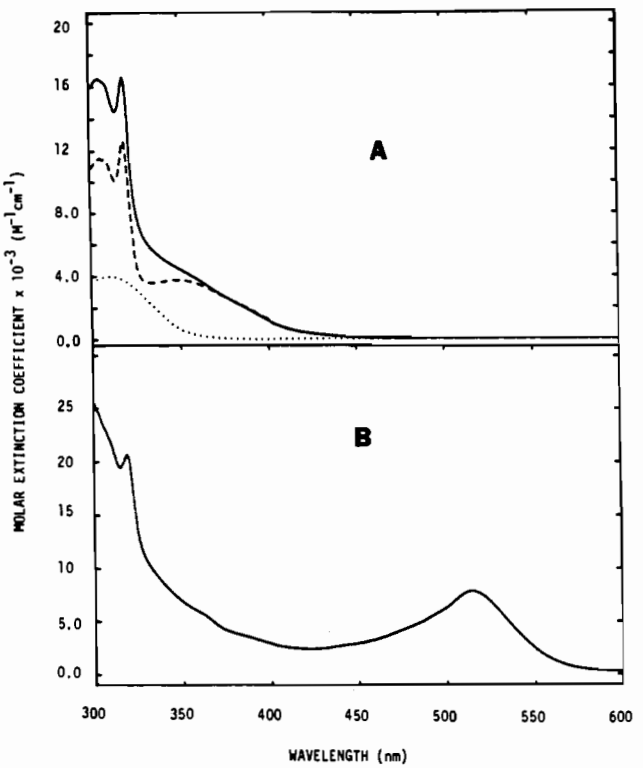

Figure 1. Absorption spectra in acetonitrile solution: (A) free py-PTZ (···), $[(bpy)Re(CO)_3(4\text{-}Etpy)](PF_6)$ (---), and $[(bpy)Re(CO)_3(py\text{-}PTZ)](PF_6)$ (—); (B) $[(bpy)Re(CO)_3(py\text{-}PTZ^{\bullet+})]^{2+}$ run immediately upon addition of excess Br_2 in acetonitrile solution.

arise from $\pi^*(bpy) \leftarrow d\pi$ transitions. For the two Ru complexes, the bpy-based MLCT transition energies and their molar extinction coefficients are approximately equal to those for the pyridine analogues.[16]

The absorption spectra of py-PTZ, $[(bpy)Re(CO)_3(py\text{-}PTZ)]^+$, and the model 4-Etpy complex in acetonitrile solution are depicted in Figure 1A. A spectral comparison shows that the spectrum of the chromophore–quencher (CQ) complex is approximately the sum of the spectra for the py-PTZ ligand and the model complex. The bpy-based MLCT band for the CQ complex appears as a broad shoulder centered at ca. 350 nm because of the contribution to the absorption spectrum of py-PTZ in that region. The spectra of the Re complexes in the ultraviolet consist of bands from intraligand transitions and from higher $\pi^*(bpy) \leftarrow d\pi$ transitions. The absorption bands at 308 and 320 nm for the model complex probably consist largely of contributions from bpy-based $\pi_1^* \leftarrow \pi$ transitions[17] and the bands at ~250 nm consist of a contribution from $\pi_2^* \leftarrow \pi$ transitions.

The Re–CQ complex was oxidized in CH_3CN both electrochemically (at $E_{app} > 1.0$ V) and chemically by using Br_2. The spectrum of the oxidized product taken immediately after oxidation is shown in Figure 1B. The obvious feature of note is the appearance of the additional, intense band at 514 nm, which is a characteristic band for PTZ-type radical cations.[18] The spectral comparisons show that 1-electron oxidation leads to oxidation at the chemically linked PTZ ligand

$$[(bpy)Re(CO)_3(py\text{-}PTZ)]^+ \xrightarrow{-e^-} [(bpy)Re(CO)_3(py\text{-}PTZ^{\bullet+})]^{2+}$$

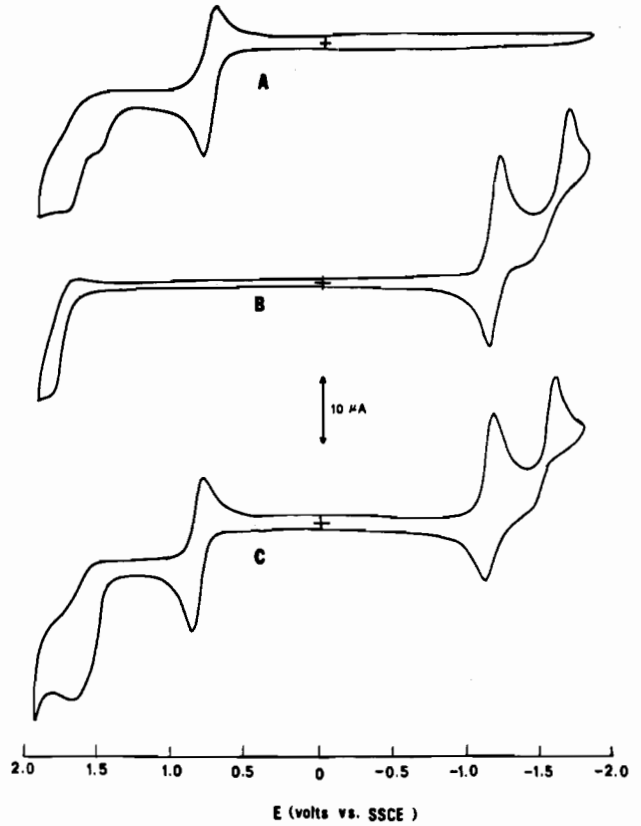

Figure 2. Cyclic voltammograms (V vs. SSCE) in acetonitrile solutions (0.1 M $NEt_4(PF_6)$): (A) py-PTZ ligand; (B) $[(bpy)Re(CO)_3(4\text{-}Etpy)](PF_6)$; (C) $[(bpy)Re(CO)_3(py\text{-}PTZ)](PF_6)$. The voltammograms were conducted by using Pt-bead working and Pt-wire auxiliary electrodes with a complex concentration of approximately 1×10^{-3} M at a scan rate of 100 mV s^{-1}.

Unfortunately, the oxidized form of the complex decomposes in solution on a time scale of minutes. We have not characterized the decomposition product but from known chemistry it could involve nucleophilic substitution on the PTZ ring[18d] and/or N–C bond cleavage between the phenothiazine ring and the 4-picolyl group. The latter reaction was suggested to be the origin of the instability of the 10-benzyl-3,7-dioctylphenothiazine radical cation in a previous study.[19]

Electrochemistry. Redox potentials for the complexes measured by CV are tabulated in Table I. Cyclic voltammograms for the py-PTZ ligand and the 4-Etpy and py-PTZ complexes of Re are presented in Figure 2. The voltammogram for the Re–CQ complex is essentially a superposition of those for the free ligand and the model complex. A chemically irreversible oxidation wave[20,21] appears at 1.6 V for the Re(II)/Re(I) couple and a chemically and electrochemically nearly reversible oxidation wave (ΔE_p = 70 mV at a scan rate of 100 mV/s) appears at 0.83 V for the $PTZ^{+/0}$ couple. The reversible reduction wave at −1.13 V is a bpy-based reduction, and the totally irreversible wave at $E_{p,c}$ = −1.48 V is due to reduction of Re(I).[20] The CV of $[(bpy)_2Ru(ACN)(py\text{-}PTZ)]^{2+}$ has the same general features as the Re complex with a distinct PTZ oxidation wave observed at 0.83 V and the Ru-based oxidation and bpy-based reductions occurring at essentially the same potentials as in the pyridine analogue.[16]

For $[(bpy)_2RuCl(py\text{-}PTZ)]^+$, the oxidation wave at ~0.83 V is actually two overlapping one-electron oxidation waves arising

(16) Durham, B.; Walsh, J. L.; Carter, C. L.; Meyer, T. J. *Inorg. Chem.* **1980**, *19*, 860.
(17) (a) Bryant, G. M.; Fergusson, J. E.; Powell, H. K. J. *Aust. J. Chem.* **1971**, *24*, 259. (b) Bryant, G. M.; Fergusson, J. E. *Aust. J. Chem.* **1971**, *24*, 275.
(18) (a) Biehl, E. R.; Chiou, H.; Keepers, J.; Kennard, S.; Reeves, P. C. *J. Heterocycl. Chem.* **1975**, *12*, 397. (b) Alkaitis, S. A.; Beck, G.; Grätzel, M. *J. Am. Chem. Soc.* **1975**, *97*, 5723. (c) Shine, H. J.; Mach, E. E., *J. Org. Chem.* **1965**, *30*, 2130. (d) Bodea, C.; Silberg, I. *Adv. Heterocycl. Chem.* **1968**, *9*, 321.
(19) Burrows, H. D.; Kemp, T. J.; Welbourn, M. J. *J. Chem. Soc., Perkin Trans. 2* **1973**, 969.
(20) Luong, J. C.; Nadjo, L.; Wrighton, M. S. *J. Am. Chem. Soc.* **1978**, *100*, 5790.
(21) Sullivan, B. P.; Bolinger, C. M.; Conrad, D.; Vining, W. J.; Meyer, T. J. *J. Chem. Soc., Chem. Commun.* **1985**, 1414.

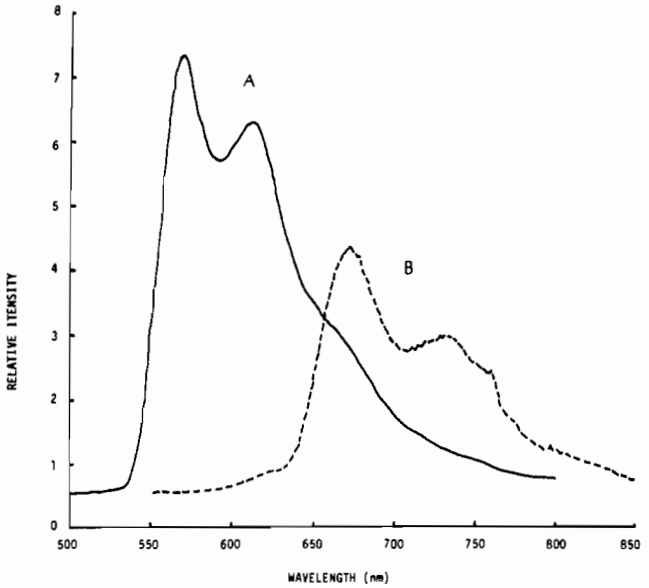

Figure 3. Corrected emission spectra in 4:1 EtOH/MeOH solution at 77 K obtained in a finger Dewar for the following Ru complexes: (A) $[(bpy)_2Ru(CH_3CN)(py\text{-}PTZ)](PF_6)_2$ (—). (B) $[(bpy)_2RuCl(py\text{-}PTZ)](PF_6)$ (---). Excitation wavelengths were at the maxima of the MLCT bands, 440 nm for A and 500 nm for B.

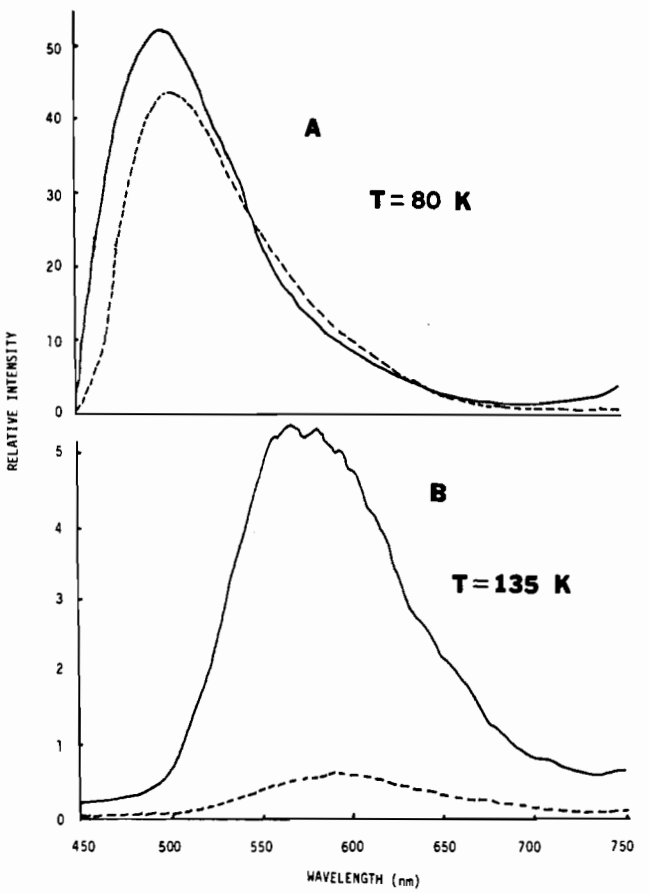

Figure 4. Corrected emission spectra in 4:1 EtOH/MeOH solution using an Oxford Cryostat for $[(bpy)Re(CO)_3(4\text{-}Etpy)](PF_6)$ (—) and $[(bpy)Re(CO)_3(py\text{-}PTZ)](PF_6)$ (---): (A) 80 K; (B) 135 K. The absorbance at the excitation wavelength, 385 nm, was 0.12 for both complexes. Note that the intensity scale for B is smaller than that for A by a factor of 10.

from the Ru(III)/Ru(II) and $PTZ^{+/0}$ couples. The peak to peak splitting is ΔE_p = 125 mV in this complex while the PTZ-based oxidation waves in the other two complexes occurred with ΔE_p = 70 mV under the same experimental conditions. The appearance of two overlapping 1-electron waves is an expected result since for the Ru(III)/Ru(II) couple of $[(bpy)_2Ru(py)Cl]^+$ $E_{1/2}$ = 0.76 V[16] under the same conditions. We were unable to obtain reliable coulometric data for the Ru–CQ complex because of the decomposition of the py-PTZ radical cation after oxidation. However, as expected for a 2-electron oxidation

$$[(bpy)_2Ru^{II}Cl(py\text{-}PTZ)]^+ \xrightarrow{-2e^-} [(bpy)_2Ru^{III}Cl(py\text{-}PTZ^{\bullet+})]^{3+}$$

addition of Br_2 in excess leads to loss of the low-energy Ru(II)-based MLCT bands at 500 nm and the appearance of a band at 514 nm for $-PTZ^{\bullet+}$. Attempts to exploit possible differences in solvent dependence for the two couples to resolve them were unsuccessful; only a single, broad wave was observed in acetonitrile, nitrobenzene, or dichloromethane as solvent.

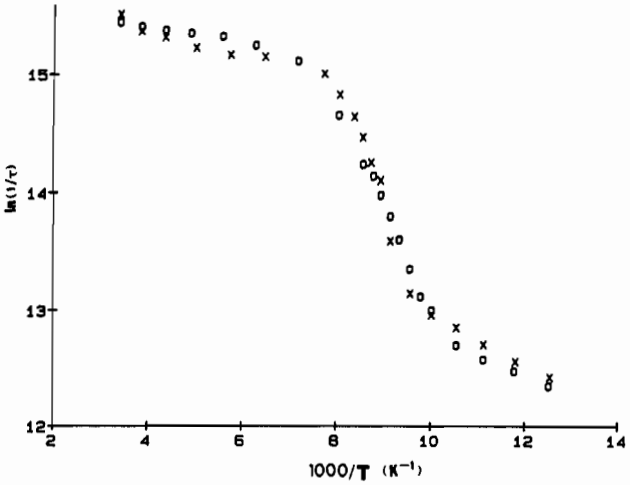

Figure 5. Temperature-dependent lifetimes in 4:1 EtOH/MeOH solution for $[(bpy)Re(CO)_3(4\text{-}Etpy)]^+$ (○) and $[(bpy)Re(CO)_3(py\text{-}PTZ)]^+$ (×). The excitation wavelength was 337 nm for both complexes.

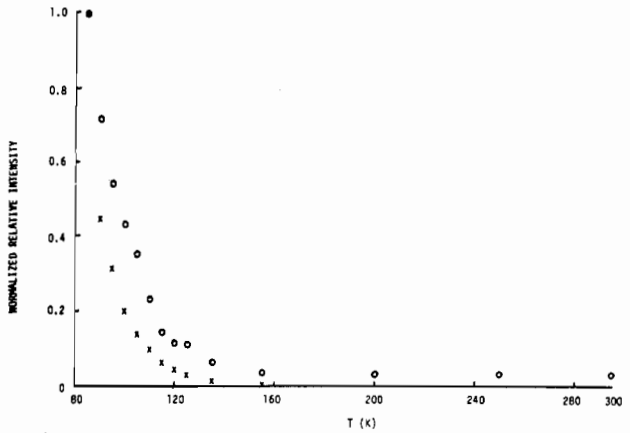

Figure 6. Normalized relative emission intensity as a function of temperature in 4:1 EtOH/MeOH solution for $[(bpy)Re(CO)_3(4\text{-}Etpy)]^+$ (○) and $[(bpy)Re(CO)_3(py\text{-}PTZ)]^+$ (×). They are plotted as $I(T)/I(85)$, where $I(T)$ and $I(85)$ are the heights of the emission maxima at temperature T and 85 K, respectively. No correction has been made for variations in bandwidth and other factors that vary with temperature.

Emission Spectra and Luminescence Lifetimes. Corrected emission spectra for the two Ru complexes at 77 K are presented in Figure 3 and for the 4-Etpy and py-PTZ complexes of Re at 80 and 135 K in Figure 4. The excitation energies for Ru complexes were at the maxima of their lowest MLCT bands, but those for Re complexes were at 385 nm in order to avoid excitation of intraligand transitions at PTZ. All three CQ complexes emit strongly at low temperatures at the same energies as their pyridine analogues. The well-resolved vibrational structure for the Ru complexes at $h\nu$ = ~1300 cm^{-1} has its origin in skeletal vibrations at bpy and indicate that the emission is from bpy-based MLCT states.[22] The emission spectra for the Re complexes are broad

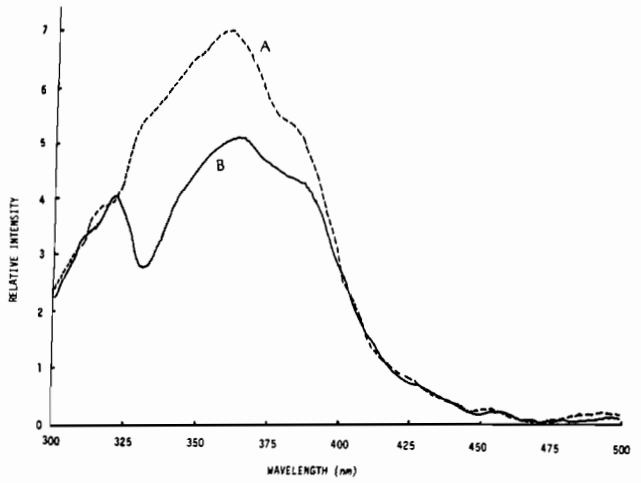

Figure 7. Corrected excitation spectra for the Re complexes in 4:1 EtOH/MeOH solution at 80 K recorded as an intensity ratio compared to the spectrum of Rhodamine B in ethylene glycol (5×10^{-3} M): (A) $[(bpy)Re(CO)_3(py\text{-}PTZ)]^+$ (---) (B) $[(bpy)Re(CO)_3(4\text{-}Etpy)]^+$ (—). Both spectra were obtained in solutions contained in glass cuvettes that had absorbances of 0.12 at 385 nm for a monitoring emission wavelength of 510 nm. The fall off in intensity below 325 nm is largely because of absorption by the glass cuvette.

and unresolved. None of the CQ complexes emit in fluid solution at room temperature.

Temperature-dependent emission lifetimes and normalized relative emission intensities for the two Re complexes in 4:1 (v/v) EtOH/MeOH are presented in Figures 5 and 6. The normalized relative emission intensities are plotted as $I(T)/I(85)$ where $I(T)$ and $I(85)$ are the heights of the emission maxima at temperatures T and 85 K, respectively. Emission intensities fall off for both complexes in the glass to fluid transition region. However, the 4-Etpy complex remains a relative strong emitter ($\phi_e \sim 0.18$ at room temperature in CH_2Cl_2)[10] from the transition region to room temperature. For all practical purposes the emission of the py-PTZ complex gradually disappears as the glass softens and becomes fluid at ~130 K. The residual emission in the lifetime measurements in fluid solution for the Re-CQ complex in Figure 5 arises from an impurity luminescence. The impurity does not appear to be a photochemical decomposition product since repeated flashes on the same sample do not result in a noticeable change in emission intensity in the solution. An attempted purification by chromatography on a silica gel column using 35% acetonitrile toluene as eluant, which separates the py-PTZ complex from the 4-Etpy complex, did not result in a significant change in luminescent properties. From its emission characteristics and the temperature-dependent lifetime data in Figure 5 in fluid solution, it seems clear that the impurity is a complex of the type $[(bpy)Re(CO)_3L]^+$.

Excitation Spectra. Corrected excitation spectra for the two Re complexes are presented in Figure 7. The spectra were obtained at 80 K in 4:1 EtOH/MeOH at emission λ_{max} (510 nm) as a ratio with that of Rhodamine B in glycerol at room temperature. The excitation spectrum of $[(bpy)Re(CO)_3(4\text{-}Etpy)]^+$ at room temperature obtained at the emission maximum of 580 nm has the same features as the spectrum at 80 K. The intensity differences between the two spectra will be discussed further in a later section.

Transient Absorption Spectra. Absorption spectra obtained as differences in absorbance before and immediately following laser excitation are presented for $[(bpy)Re(CO)_3(py\text{-}PTZ)]^+$ and

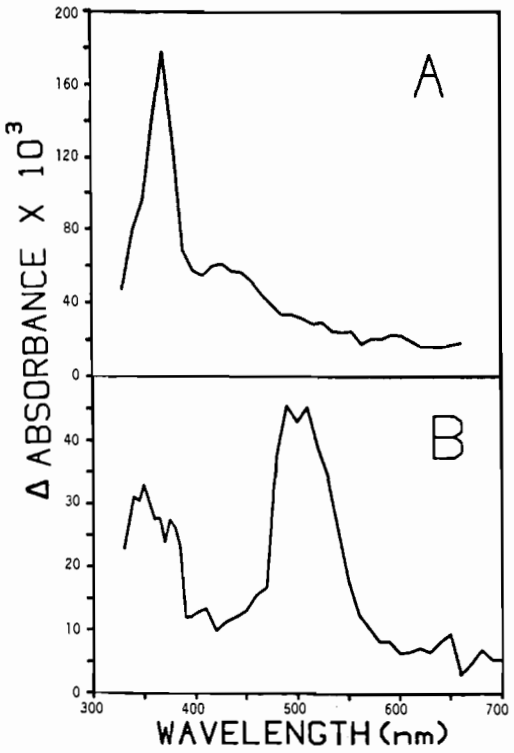

Figure 8. Transient absorption spectra in acetonitrile solution showing the difference in absorbance before and immediately following laser flash photolysis: (A) $[(bpy)Re(CO)_3(4\text{-}Etpy)]^+$; (B) $[(bpy)Re(CO)_3(py\text{-}PTZ)]^+$. Both spectra were obtained in solutions containing sufficient complex that the ground-state absorbance was 0.5 at the excitation wavelength, 355 nm. The laser pulse energy was 10 mJ/pulse, and the delay times were 50 ns for A and 25 ns for B.

$[(bpy)Re(CO)_3(4\text{-}Etpy)]^+$ in CH_3CN solvent in Figure 8. Following the flash, the TA spectrum of the 4-Etpy complex shows an absorbance increase with $\lambda_{max} \sim 370$ nm. In the TA spectrum of the CQ complex an absorption feature appears at ~500 nm with a less intense feature at ~350 nm. The significant difference in the TA spectra for the two Re complexes is noteworthy as is the significantly decreased absorptivity for the CQ complex, which is, in part, a consequence of its short lifetime (25 ns).

Transient absorption (TA) experiments were also conducted for $[(bpy)_2Ru(ACN)(py\text{-}PTZ)]^{2+}$ in acetonitrile at room temperature. However, no TA signal was observed and if a transient exists its lifetime must be short on the time scale of the laser pulse (<10 ns).

The appearance of the absorption feature at 500 nm occurs within the laser pulse in the nanosecond TA experiment. We have observed the appearance of the intermediate absorbing at 500 nm using picosecond transient techniques by measuring the rise kinetics of the $PTZ^{+\cdot}$ signal at 500 nm in several different solvents. Figure 9 shows the $\Delta(OD(t))$ response at 500 nm following 30-ps excitation in DMF and CH_2Cl_2. Figure 9A shows the rise of the transient signal in DMF. The absorption temporal profile in DMF provides clear evidence for two processes, one occurring during the laser pulse and a slower process that can be time-resolved. The smooth line in Figure 9A shows the computer-calculated best fit to eq 3. The parameters indicate the presence of a "prompt" component generated during the laser pulse that accounts for 47% of the signal and a temporally resolved "slow" component that accounts for 53% of the signal with $\tau_{rise} = 240$ ps. Similar observations were made at 500 nm in polar solvents with low polarizability such as acetone, acetonitrile, Me_2SO, methanol, and *N*-methylformamide. In $CHCl_3$ and CH_2Cl_2 the transient absorbance signal develops almost entirely during the 30-ps laser pulse. Analysis of the rise kinetics (smooth line, Figure 9B) shows that 88% of the signal appears during the laser pulse while 12% of the absorbance grows in slowly with an approximate $\tau_{slow} = 390$ ps. Results obtained from the transient kinetics based on eq 3 are collected in Table II.

(22) (a) Klassen, D. M.; Crosby, G. A. *J. Mol. Spectrosc.* **1968**, *26*, 72. (b) Crosby, G. A.; Watts, R. J.; Carstens, D. H. W. *Science (Washington, D.C.)* **1970**, *170*, 1195. (c) Caspar, J. V. Ph.D. Dissertation, University of North Carolina at Chapel Hill, 1982. (d) Caspar, J. V.; Meyer, T. J. *Inorg. Chem.* **1983**, *22*, 2444. (e) Caspar, J. V.; Westmoreland, T. D.; Allen, G. H.; Bradley, P. G.; Meyer, T. J. *J. Am. Chem. Soc.* **1984**, *106*, 3492. (f) Kober, E. M.; Meyer, T. J. *Inorg. Chem.* **1985**, *24*, 106.

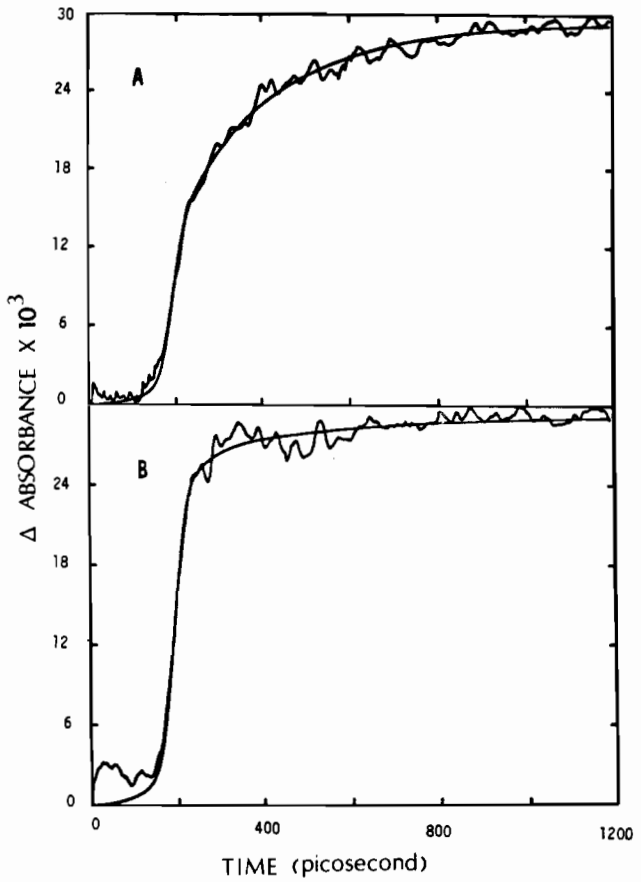

Figure 9. Transient absorption signals produced by 355 nm laser excitation (0.5 mJ, 30-ps fwhm) for $[(bpy)Re(CO)_3(py\text{-}PTZ)]^+$ monitored at the $PTZ^{\bullet+}$ absorption maximum (500 nm): (A) DMF solvent; (B) CH_2Cl_2 solvent. Noisy curves represent an average of 1000 shots; smooth curves are calculated best fits to the data (see text for fitting parameters).

Table II. Kinetic Parameters at Room Temperature for Absorbance Rise Times at 500 nm[a]

solvent	α_{slow}	τ_{slow}, ps	α_{prompt}	$10^{-9}k_q$, s^{-1}
acetone	0.52	201	0.48	5.0
acetonitrile	0.58	207	0.42	4.8
chloroform	0.21	121	0.79	
dimethyl sulfoxide	0.52	212	0.48	4.7
dimethylformamide	0.53	245	0.47	4.1
methylene chloride	0.12	391	0.88	
methanol	0.51	182	0.49	5.5
N-methylformamide	0.45	193	0.55	5.2

[a] Calculated by computer fitting the experimental data to $\Delta A(t) = \alpha_{slow}\exp\{t/\tau_{slow}\} + \alpha_{prompt}A_{prompt}$, where $\alpha_{prompt}A_{prompt}$ is the component in the absorbance change that occurs during the laser pulse.

The decay rate of the charge-separated state, $[(bpy^{\bullet-})Re^{I}(CO)_3(py\text{-}PTZ^{\bullet+})]^+$, is 4.0×10^7 s^{-1} in acetonitrile at room temperature as measured in the TA experiments.

The related bimolecular, outer-sphere process using the 4-Etpy complex, $[(bpy)Re(CO)_3(4\text{-}Etpy)]^+$, and 10-methylphenothiazine (10-MePTZ) was studied in acetonitrile by conventional flash photolysis. Following flash excitation and quenching

$$[(bpy)Re^{I}(CO)_3(4\text{-}Etpy)]^+ \xrightarrow{h\nu} [(bpy^{\bullet-})Re^{II}(CO)_3(4\text{-}Etpy)]^{+*}$$

$$[(bpy^{\bullet-})Re^{II}(CO)_3(4\text{-}Etpy)]^{+*} + 10\text{-}MePTZ \rightarrow [(bpy^{\bullet-})Re^{I}(CO)_3(4\text{-}Etpy)]^0 + 10\text{-}MePTZ^+$$

back electron transfer

$$[(bpy^{\bullet-})Re^{I}(CO)_3(4\text{-}Etpy)]^0 + 10\text{-}MePTZ^+ \rightarrow [(bpy)Re(CO)_3(4\text{-}Etpy)]^+ + 10\text{-}MePTZ \quad (4)$$

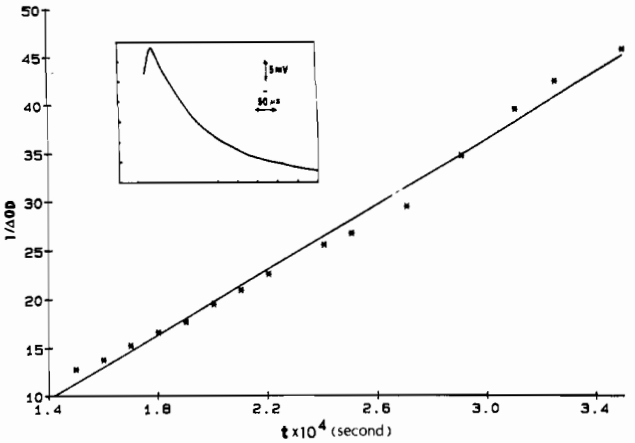

Figure 10. The best fit to the second-order kinetics (solid line) of the decay signal (asterisks denote experimental data) at 514 nm produced by a broad-band flash with a cutoff filter of 360 nm in a freeze–thaw–pump degassed acetonitrile solution containing $[(bpy)Re(CO)_3(4\text{-}Etpy)]^+$ (5.0×10^{-5} M) and 10-methylphenothiazine (1.0×10^{-3} M). $\Delta(OD)$ was calculated by $\Delta(OD) = \log\{I_0/(I_0 + \Delta I)\}$ where I_0 is the intensity before the flash and ΔI is the change of intensity induced by the flash. An oscilloscope trace is shown in the insert.

was monitored at 514 nm and the transient response fit to second-order, equal concentration kinetics as shown in Figure 10. Some curvature was noted in the plots, and the solutions were not completely photochromic, possibly caused by ligand-loss chemistry in the reduced Re complex.[23,24]

The observed rate constant (k_{obsd}) for reaction 4 calculated from the slope of the kinetic plots, using a molar extinction coefficient change of 8010 cm^{-1} M^{-1} at 514 nm, is 1.3×10^{10} M^{-1} s^{-1}. This reaction is diffusion-controlled given that the diffusion rate constant for related reactions[25] in acetonitrile is $\sim 2 \times 10^{10}$ M^{-1} s^{-1}, and k_{obsd} (1.3×10^{10} M^{-1} s^{-1}) is the lower limit of the chemically activated component of the electron-transfer rate in reaction 4. It is notable that this rate constant is 3 orders of magnitude faster than the decay of the charge-separated state in the Re–CQ complex where the quencher, PTZ, is chemically attached.

Discussion

The results outlined here lead to some important conclusions concerning the nature of the thermally equilibrated excited states in $[(bpy)Re(CO)_3(py\text{-}PTZ)]^+$ compared to the model 4-Etpy complex and, by inference, give insight into the pattern of photophysical events that occur following excitation. It is clear that the photophysical properties of the complexes are essentially the same in the glass but are profoundly different in fluid solution. We begin with a discussion of the electronic structures of the complexes followed by a detailed consideration of the photophysical properties of the Re–CQ complex. Because of our ability to observe transient behavior and direct evidence for intramolecular electron transfer for the Re-based but not the Ru-based py-PTZ complexes, the majority of our efforts have been centered on the Re complex.

Chromophore–Quencher Complexes. The absorption spectra for the Re and Ru chromophore–quencher complexes based on py-PTZ are within experimental error the sum of the separate PTZ and $Ru^{II}(bpy)$- or $Re^{I}(bpy)$-based chromophores. The absorption spectra show that electronic interactions between the two different types of chemical sites are weak, as expected, given the methylene bridge that separates the PTZ group from the metal based chromophores. In Figure 11 are illustrated three different rotational configurations around the $-CH_2-$ link for the Re complex. The two chemical sites are well-separated from each

(23) Summers, D. P.; Luong, J. C.; Wrighton, M. S. *J. Am. Chem. Soc.* **1981**, *103*, 5238.
(24) Fredericks, S. M.; Wrighton, M. S. *J. Am. Chem. Soc.* **1980**, *102*, 6166.
(25) Bock, C. R.; Connor, J. A.; Gutierrez, A. R.; Meyer, T. J.; Whitten, D. G.; Sullivan, B. P.; Nagle, J. K. *J. Am. Chem. Soc.* **1979**, *101*, 4815.

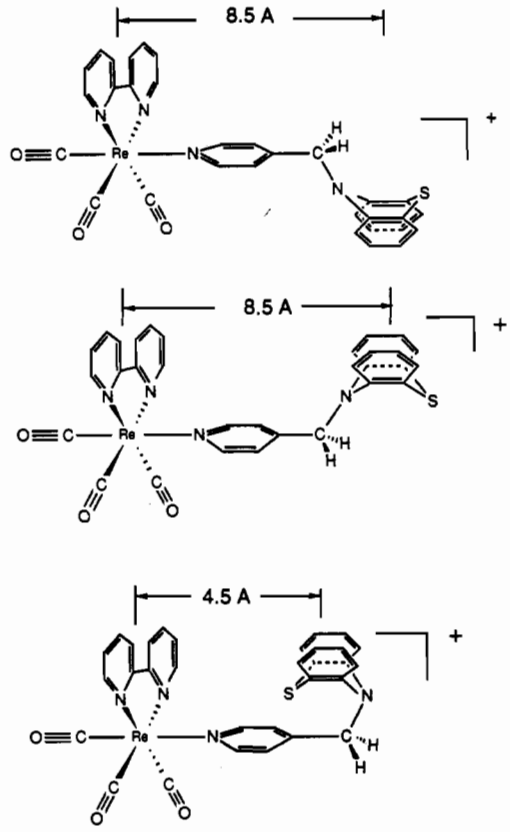

Figure 11. Structures of $[(bpy)Re(CO)_3(py\text{-}PTZ)]^+$ illustrating three different rotational configurations around the $-CH_2-$ link to the complex.

other in what are expected to be the most stable configurations.

The electrochemical results further substantiate the existence of weakly interacting –PTZ-based and metal complex-based sites. For all complexes, the PTZ-based oxidations occur at 0.83 V, which is 70 mV higher than that for the free ligand. Oxidation at Re(I) and reduction at bpy in the Re CQ complex are shifted to lower potentials by 120 and 50 mV from those in the 4-Etpy complex, respectively.

A disappointing feature of the complexes is the long-term instability of the –PTZ-oxidized form. Because of the instability we did not obtain spectroscopic evidence for the low-energy MLCT or LMCT charge-transfer transitions between the metal and PTZ-based redox sites, e.g.

$$[(bpy)_2Ru^{II}Cl(py\text{-}PTZ^{\bullet+})]^{2+} \xrightarrow{h\nu} [(bpy)_2Ru^{III}Cl(py\text{-}PTZ)]^{2+}$$

analogous to metal to metal charge-transfer (MMCT) transitions in mixed-valence dimers[3,4]

$$\left[(bpy)_2ClRu^{II}\text{–}N\text{–}N\text{–}Ru^{III}Cl(bpy)_2\right]^{3+} \xrightarrow{h\nu}$$

$$\left[(bpy)_2ClRu^{III}\text{–}N\text{–}N\text{–}Ru^{II}Cl(bpy)_2\right]^{3+}$$

nor to search for oxidative, intramolecular electron-transfer quenching, e.g.

$$[(bpy)Re(CO)_3(py\text{-}PTZ^{\bullet+})]^{2+} \xrightarrow{h\nu} [(bpy^{\bullet-})Re^{II}(CO)_3(py\text{-}PTZ^{\bullet+})]^{2+*} \rightarrow [(bpy)Re^{II}(CO)_3(py\text{-}PTZ)]^{2+}$$

The singly oxidized chromophore-based Ru complex $[(bpy)_2ClRu(py\text{-}PTZ)]^{2+}$ is especially interesting in this regard since the electrochemical measurements show that the Ru(III)/Ru(II) and $-PTZ^{+/0}$ couples occur at nearly the same potential and the free energy difference between the oxidation state isomers is ~0.

As shown by the similarities in emission band shapes and energies (Figure 4) and lifetimes (Figure 5) between $[(bpy)Re(CO)_3(4\text{-}Etpy)]^+$ and $[(bpy)Re(CO)_3(py\text{-}PTZ)]^+$ at 80 K, the presence of the PTZ group also leaves the photophysical characteristics of the lowest lying, emitting MLCT states unaffected. Nonetheless, as indicated by the excitation spectra in Figure 7, the PTZ group does play an interesting role in the overall photophysical properties of the molecule. At least qualitatively, the excitation spectrum for $[(bpy)Re(CO)_3(4\text{-}Etpy)]^+$ follows the absorption spectrum in that the excitation peaks at 323 and 366 nm follow absorption features at 322 and 354 nm in alcohol solution.

For the py-PTZ complex, there is a marked increase in emission intensity in the region of PTZ-based $\pi \rightarrow \pi^*$ absorption centered at ~320 nm. The excitation spectrum provides clear evidence for intramolecular sensitization of the emitting MLCT state by $^1(\pi\pi^*)$ or $^3(\pi\pi^*)$ states of PTZ. Intramolecular energy transfer is a spontaneous process given the energies of the lowest $^3(\pi\pi^*)$ state for PTZ (2.64 eV[26]) and ^{3}(MLCT) for the Re-based chromophore (2.14 eV).

The appearance of the intramolecular sensitization process is interesting in its own right. It shows that an attached organic chromophore can be used to "fill in" the absorption spectrum of the molecular ensemble without significant perturbation of the reactive MLCT state.

Intramolecular Electron-Transfer Quenching in $[(bpy)Re(CO)_3(py\text{-}PTZ)]^+$. Although the emission and lifetime characteristics of the py-PTZ and 4-Etpy complexes are nearly interchangeable at 80 K in the glass, as shown by emission intensity data in Figure 6, they change dramatically as the glass softens and the glass to fluid transition region is approached. The emission intensity for the 4-Etpy complex decreases considerably in this region, but the complex continues to emit at higher temperatures and is a reasonable emitter even at room temperature ($\phi_e = 0.18$ in CH_2Cl_2).[10] The loss of emission intensity for the 4-Etpy complex is paralleled by a decrease in lifetime (Figure 5) and a shift to lower energy and is understandable based on recently documented ideas on related systems[27] where (1) the decrease in emission energy with increasing temperature is a consequence of solvent dipole reorientation responding to the change in electronic configurations between the ground and excited states, (2) the decrease in lifetime as the emission energy decreases is a consequence of an increase in the rate constant for nonradiative decay (k_{nr}), which varies as $\ln k_{nr} \propto -E_{em}$ (E_{em} is the emission maximum) as predicted by the energy gap law.[28]

The change in emission intensity with temperatures for the py-PTZ complex is more profound. As the glass softens over the narrow temperature range of 100–130 K, the excited-state emission disappears and the lifetime shortens. The quenching process is essentially completed by 155 K when the glass is fully fluid. A closely related observation has been made for the oxidative chromphore-quencher complex[6b]

$$[(bpy)Re(CO)_3(N\text{–}\langle\rangle\text{–}N^+CH_3)]^{2+}$$

where following initial Re → bpy MLCT excitation, oxidative, intramolecular electron-transfer quenching is induced in the glass to fluid transition region.

The room-temperature TA spectrum for the Re(py-PTZ) complex in Figure 8 shows that the net result of MLCT quenching

(26) (a) Moroi, Y.; Braun, A. M.; Grätzel, M. *J. Am. Chem. Soc.* **1979**, *101*, 567. (b) Maestri, M.; Grätzel, M. *Ber. Bunsenges. Phys. Chem.* **1977**, *81*, 504.
(27) (a) Lumpkin, R. S.; Meyer, T. J. *J. Phys. Chem.* **1986**, *90*, 5307. (b) Danielson, E.; Lumpkin, R. S.; Meyer, T. J. *J. Phys. Chem.*, in press. (c) Barigelletti, F.; Belser, P.; Zelewsky, A. V.; Juris, A.; Balzani, V. *J. Phys. Chem.* **1985**, *89*, 3680. (d) Kitamura, N.; Kim, H.-B.; Kawanishi, Y.; Obata, R.; Tazuke, S. *J. Phys. Chem.* **1986**, *90*, 1488.
(28) (a) Caspar, J. V.; Sullivan, B. P.; Kober, M. D.; Meyer, T. J. *Chem. Phys. Lett.* **1982**, *91*, 91. (b) Kober, E. M.; Caspar, J. V.; Lumpkin, R. S.; Meyer, T. J. *J. Phys. Chem.* **1986**, *90*, 3722. (c) Meyer, T. J. *Pure Appl. Chem.* **1986**, *58*, 1193.

Scheme I

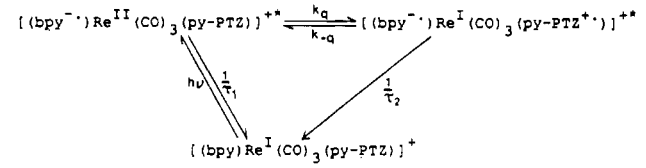

in $[(bpy)Re(CO)_3(py\text{-}PTZ)]^+$ is the same but involves *reductive* intramolecular electron-transfer quenching to give the charge separated state $[(bpy^{\bullet-})Re^{I}(CO)_3(py\text{-}PTZ^{\bullet+})]^+$. The evidence for the charge-separated state is clear from the appearance of the intense absorption feature at ~500 nm for $-PTZ^+$, which also includes a contribution from a bpy$^{\bullet-}$-based $\pi \rightarrow \pi^*$ transition on Re(I).[29] In addition, when compared to $[(bpy^{\bullet-})Re^{II}(CO)_3(4\text{-}Etpy)]^{+*}$, the broadening and blue shift in the absorption feature at 350 nm for the py-PTZ complex is also consistent with the appearance of a charge-separated state. The same spectral differences, at least in qualitative terms, exist between the absorption spectra of $[(bpy)_2Ru^{III}(bpy^{\bullet-})]^{2+*}$ and $[(bpy)_2Ru^{II}(bpy^{\bullet-})]^+$ where λ_{max} for the lowest energy bpy-based $\pi \rightarrow \pi^*$ transitions are at 370 and 343 nm in acetonitrile.[29,30] The similarity in the spectral shift for the Re complexes with the shift in $\pi \rightarrow \pi^*$ transition energies for $[(bpy)_2Ru^{III}(bpy^{\bullet-})]^{2+*}$ and $[(bpy)_2Ru^{II}(bpy^{\bullet-})]^+$ is consistent with a bpy$^{\bullet-}$ radical anion bound to Re(I) in the charge-separated state rather to Re(II) as is the case in the MLCT state.

The picosecond transient experiments at room temperature provide direct evidence for the growth of the charge-separated state $[(bpy^{\bullet-})Re(CO)_3(py\text{-}PTZ^{\bullet+})]^{+*}$. Those data, combined with the appearance of the MLCT-based emission at 80 K, complete MLCT quenching by 155 K, and the appearance of the charge-separated state are consistent with the intramolecular quenching scheme given in Scheme I.

Before discussing the kinetic quenching scheme in further detail, it is of interest to note the following details. (1) The intramolecular quenching step (k_q) produces an organic donor–acceptor "exciplex" chemically linked by a Re(I) bridge. (2) The excitation–quenching sequence, $h\nu$ followed by k_q, results in the intramolecular sensitization of a low-lying interligand charge-transfer (ILCT) excited state.[31] An absorption band arising from direct ligand → ligand excitation

$$[(bpy)Re(CO)_3(py\text{-}PTZ)]^+ \xrightarrow{h\nu} [(bpy^{\bullet-})Re(CO)_3(py\text{-}PTZ^{\bullet+})]^{+*}$$

is not observed in the absorption spectrum because of negligible electronic coupling between PTZ and bpy. Also, we have been unable to observe emission from the ILCT "exciplex" excited state.

From experimental measurements in alcohol solution, $1/\tau_1$, which is the sum of the radiative (k_r) and nonradiative (k_{nr}) decay constants for the MLCT state, is expected to be approximately equal to that of the model complex $1/\tau_0$ (τ_0 = 213 ns; $k_0 = 4.7 \times 10^6$ s^{-1}). From the picosecond experiments k_q (4.0×10^9 s^{-1}) is much more rapid because of intramolecular quenching, and from the laser flash result, $k_2 = 1/\tau_2 = 4.0 \times 10^7$ s^{-1}. In the absence of competing processes, it is clear that the intramolecular quenching rate is sufficiently rapid that the ILCT state must be formed in high efficiency. On the basis of the absorbance changes in Figure 8 with the data for $\pi \rightarrow \pi^*$ transitions of bpy$^{\bullet-}$ in $Ru(bpy)_3^{2+*}$ [30] and $Ru(bpy)_3^+$,[29] the per photon absorbed quantum yield of formation of the charge-separated state is estimated to be ~74%.[32] Further, that excited state concentrations calculated from the absorbance changes at 343 and 514 nm, which arise mainly from bpy$^{\bullet-}$-based and PTZ$^{\bullet+}$-based $\pi \rightarrow \pi^*$ transitions, respectively, are within 10% of each other further substantiates the proposed formulation of the charge-separated state.[32]

Scheme II

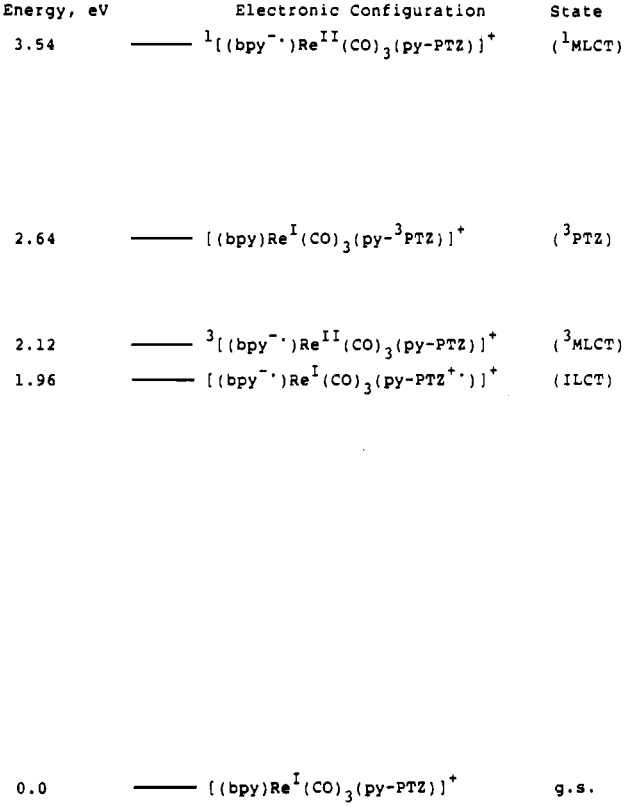

(29) Heath, G. A.; Yellowlees, L. J.; Braterman, P. S. *J. Chem. Soc., Chem. Commun.* **1981**, 287.

(30) (a) Creutz, C.; Chou, M.; Netzel, T. L.; Okumura, M.; Sutin, N. *J. Am. Chem. Soc.* **1980**, *102*, 1309. (b) Milder, S. J.; Gold, J. S.; Kliger, D. S. *J. Phys. Chem.* **1986**, *90*, 548. (c) Lachish, U.; Infelta, P. P.; Grätzel, M. *Chem. Phys. Lett.* **1979**, *62*, 317. (d) Braterman, P. S.; Harriman, A.; Heath, G. A.; Yellowlees, L. J. *J. Chem. Soc., Dalton Trans.* **1983**, *1801*.

(31) (a) Koester, V. J. *Chem. Phys. Lett.* **1975**, *32*, 575. (b) Truesdell, K. A.; Crosby, G. A. *J. Am. Chem. Soc.* **1985**, *107*, 1787. (c) Crosby, G. A.; Highland, R. G.; Truesdell, K. A. *Coord. Chem. Rev.* **1985**, *64*, 41.

(32) The quantum efficiency for formation of the charge-separated state relative to the efficiency of formation of the MLCT state for the 4-Etpy complex is given by

$$\phi = C^*_{CQ}(t = 0)/C^*_M(t = 0)$$

$C^*_{CQ}(t = 0)$ and $C^*_M(t = 0)$ are concentrations of the excited states for the Re CQ and the model complexes immediately after laser excitation. It is estimated by the equation

$$\Delta A(\lambda,t) = [\epsilon^*(\lambda) - \epsilon(\lambda)](C^*(t))l \qquad \text{(i)}$$

where $\Delta A(\lambda,t)$ is the observed absorbance change at wavelength λ at time t after laser excitation, $\epsilon^*(\lambda)$ and $\epsilon(\lambda)$ are the molar extinction coefficients of the excited state and the ground state, $C^*(t)$ is the concentration of the excited state, and l (1 cm) is the optical pathlength. $\Delta A(t)$ values from Figure 8 were extrapolated to $t = 0$ by using the first-order kinetic equation

$$\Delta A(\lambda,t) = \Delta A(\lambda,t = 0) \exp(-t/\tau) \qquad \text{(ii)}$$

where τ is the lifetime of the excited state. Combining eq i and ii, we can calculate the initial concentrations of the excited states following the laser pulse. Assuming that extinction coefficients for the $\pi \rightarrow \pi^*$ transitions of bpy$^{\bullet-}$ in $Re^{II}(bpy^{\bullet-})$ and $(bpy^{\bullet-})Re^{I}(py\text{-}PTZ^{\bullet+})$ are the same as in $Ru(bpy)_3^{2+*}$ ($\epsilon_{375} = 2.9 \times 10^4$ M^{-1} cm^{-1})[30] and $Ru(bpy)_3^+$ ($\epsilon_{343} = 1.43 \times 10^4$, $\epsilon_{514} \sim 1.0 \times 10^4$ M^{-1} cm^{-1}),[29] respectively, and given the known ground-state absorptions $\epsilon_{514} = 8010$ M^{-1} cm^{-1} for PTZ$^{\bullet+}$, $\epsilon_{375} = 2700$ M^{-1} cm^{-1} for the model complex, and $\epsilon_{514} \sim 0$ for the Re CQ complex, the data in Figure 8 give $C^*_M = 8.7 \times 10^{-6}$ M and $C^*_{CQ} = 6.8 \times 10^{-6}$ M (based on absorbance change at 514 nm). For the charge-separated state, the absorbance increase at 343 nm due to oxidation of the PTZ site as shown in Figure 1 is approximately compensated for by the absorbance decrease due to the loss of the MLCT transition. Therefore, the ΔA change at this wavelength has its origin in the bpy-based $\pi \rightarrow \pi^*$ transitions. On the basis of this argument, we obtain $C^*_{CQ} = 6.1 \times 10^{-6}$ M (based on absorbance change at 343 nm). The charge-separated state concentrations calculated from the absorbance changes at the two wavelengths in the TA spectrum are within 10%, and the average quantum efficiency is ~74%.

The quenching process is thermodynamically spontaneous. From the potential for the bpy-based reduction in $[(bpy)Re(CO)_3(py\text{-}PTZ)]^+$ at −1.13 V and the room-temperature emission energy for $[(bpy)Re(CO)_3(4\text{-}Etpy)]^+$ (585 nm = 2.12 eV), all in acetonitrile, the estimated potential for the excited state couple $[(bpy^{\bullet-})Re^{II}(CO)_3(py\text{-}PTZ)]^{+*}/[(bpy^{\bullet-})Re^{I}(CO)_3(py\text{-}PTZ)]$ is 0.99 V vs. SSCE. From this potential and the potential of the $PTZ^{+/0}$ couple (0.83 V), intramolecular reductive quenching is favored by 0.2–0.3 eV.

As noted above on the basis of the low-temperature excitation spectra, direct $\pi\pi^*$ excitation at py-PTZ leads to intramolecular sensitization of the emitting Re–bpy-based MLCT state. However, TA experiments monitored at 465 nm (λ_{max} for ^3PTZ[19,33]) gave no evidence for ^3PTZ as a transient. This is an expected result since the energy of ^3PTZ (2.64 eV[26]) is considerably higher than the energies of either ^3MLCT or the charge-separated ILCT state (1.96 eV). In the transient absorbance experiments, the photolysis wavelength (355 nm) was in a region where py-PTZ is essentially transparent so that ^3PTZ-initiated transient events were unimportant.

The energy level diagram shown in Scheme II is derived from our experimental observations. The energies of the ^1MLCT and ^3MLCT states were estimated by using the absorption (350 nm = 3.54 eV) and emission band maxima for the 4-Etpy complex. Since neither includes contributions to the band energies from intramolecular and solvent distortion energies, which are usually small for MLCT states, the values for ^1MLCT and ^3MLCT are upper and lower limits, respectively. In fact, given the appearance of multiple MLCT transitions in related complexes of Os(II), there are probably a series of MLCT transitions with a direct transition to the ^3MLCT-based state occurring in the low-energy tail.[34] Because of spin–orbit coupling, the pure ^1MLCT and ^3MLCT states are expected to be strongly mixed.

Intramolecular Quenching. Some interesting questions arise concerning the nature of the intramolecular quenching process: (1) At room temperature, from which state, ^1MLCT or ^3MLCT or both, is the quenching occurring? (2) Given the structures in Figure 11, what is the electron-transfer pathway at the microscopic level, through the pyridine bridge or by direct through-space overlap between Re^{II} and PTZ? (3) What is the origin of the dramatic temperature effect on quenching in the glass?

In the glass at low temperature, loss of emission from ^3MLCT provides direct evidence for intramolecular quenching. Also, the fact that quenching occurs following excitation into the low-energy part of the absorption profile, where direct excitation into ^3MLCT is a major contributor, shows that intramolecular quenching of ^3MLCT does occur. However, a contribution may also exist from intramolecular quenching of ^1MLCT before $^1MLCT \rightarrow {}^3MLCT$ interconversion can occur as indicated by the picosecond transient experiments. There are at least two processes leading to the formation of $PTZ^{\bullet+}$, a "prompt" one that occurs during the laser pulse (355 nm, 30 ps, 1 mJ/pulse) and a time-resolved, slower process. It seems clear that the slower process has its origin in intramolecular quenching of the ^3MLCT state. The "prompt" process may have its origin in electron-transfer quenching of the ^1MLCT state, which is expected to be faster than the quenching of the ^3MLCT state. However, photoejection of an electron from PTZ, which is a known process,[18b] seems the more likely origin at the laser power used (1 mJ/pulse). We hope to explore this point further by modifying the complex at the chromophoric ligand and/or at the PTZ group in such a way as to make quenching of ^3MLCT nonspontaneous.

The temperature-dependent emission data show that intramolecular quenching is triggered as the glass softens and is occurring well before the glass to fluid transition is complete at >140 K. Contributions to the vibrational barrier to electron transfer are expected to exist from PTZ-based intramolecular modes that interconvert the folded (PTZ) and planar (PTZ^+) structures,[18d,35] surrounding solvent dipoles whose orientations respond to the change in electronic configuration involved in the electron-transfer act, and, possibly, from changes in the relative orientations between the Re(II) and −PTZ sites (Figure 11). The intramolecular quenching process is spontaneous by 0.2 V, at least at room temperature. Assuming a self-exchange rate constant of $\sim 10^9$ s^{-1} for the Re(II)/Re(I) and $PTZ^{+/0}$ couples in the CQ complex and using the classical result for the free energy of activation, $\Delta G^* = (\lambda + \Delta G)^2/4\lambda$ (λ is the sum of the vibrational and solvent trapping barriers to electron transfer), we think it probable that $-\Delta G \sim \lambda$ and that the electron-transfer process is close to being barrierless. If so, the dramatic decrease in lifetime as the glass softens may be triggered by dynamical reorientational processes in the surrounding solvent or perhaps at the PTZ group.

The intramolecular quenching process is expected to be highly solvent dependent since there is a very large charge redistribution in the molecule after electron transfer and, therefore, a considerable change in the intramolecular dipole moment. An attempt to correlate the intramolecular electron-transfer rates (the slower component in the picosecond TA experiments) with solvent parameters like dipole relaxation time, static dielectric constant, refractive index, etc. was not successful. This is, in part, caused by the narrow distribution of the rate constants and the large uncertainties in the chlorinated hydrocarbon solvents. The possibility also exists that contributions from the solvent may exist in both the frequency factor and the exponential energy terms[36] for the electron transfer.

Recombination by Back Electron Transfer: Decay of the ILCT or Charge-Separated State. From the pattern of reactions in Scheme I, decay of the charge-separated excited state can occur by back electron transfer (k_{-q}) to give ^3MLCT, or direct radiative or nonradiative decay to the ground state ($1/\tau_2$). The decay (τ_2 = 25 ns) of the charge-separated state is far more rapid than the intrinsic decay ($\tau_1 \sim 213$ ns) of the ^3MLCT excited state, and $k_q >> k_{-q}$ so that back electron transfer to ^3MLCT followed by decay of ^3MLCT cannot play an important role in the observed dynamics. The absence of a detectable emission shows that $k_2 = 1/\tau_2$ is dominated by a nonradiative process that corresponds to long-range electron transfer between $bpy^{\bullet-}$ and $PTZ^{\bullet+}$.

From the reduction potential for $bpy^{-/0}$ (−1.13 V) and the oxidation potential for $PTZ^{+/0}$ (0.83 V) in $[(bpy)Re(CO)_3(py\text{-}PTZ)]^+$ the estimated free energy change for recombination by back electron transfer in the charge-separated excited state is ~2 eV. Even though the decay is highly favorable thermodynamically, the reaction is relatively slow, $k_2 = 4.0 \times 10^7$ s^{-1}. By comparison, for $[Ru(bpy)_3]^{2+*}$, which has approximately the same excited-state energy, nonradiative decay, $[(bpy^{\bullet-})Ru^{III}(bpy)_2]^{2+*} \rightarrow [(bpy)Ru(bpy)_2]^{2+}$ compared to $[(bpy^{\bullet-})Re(CO)_3(py\text{-}PTZ^{\bullet+})]^{+*} \rightarrow [(bpy)Re(CO)_3(py\text{-}PTZ)]^+$, is slower by a factor of ~10. Although ILCT excited-state decay is an electron-transfer process in the "inverted free energy region" where $|\Delta G| > \lambda$, it also is an excited-state decay process, and such factors as the energy gap law may play a role in determining the decay rates.[2a,28]

Another interesting comparison is between decay of the charge-separated state in the Re CQ complex ($k = 4.0 \times 10^7$ s^{-1}), and back electron transfer within the association complex between $[(bpy)Re(CO)_3(4\text{-}Etpy)]^0$ and 10-$MePTZ^+$ ($k > 1.3 \times 10^{10}$ s^{-1})

$$[(bpy^{\bullet-})Re(CO)_3(4\text{-}Etpy)]^0,10\text{-}MePTZ^{\bullet+} \rightarrow [(bpy)Re(CO)_3(4\text{-}Etpy)]^+,10\text{-}MePTZ$$

The two reactions occur with virtually the same ΔG change, yet the intramolecular reaction, where the relative orientation of the electron donor and acceptor is restricted, is *slower* by 3 orders of magnitude than the reaction within the association complex. The large decrease in rate constant for the intramolecular case

(33) Henry, B. R.; Kasha, M. *J. Chem. Phys.* **1967**, *47*, 3319.
(34) (a) Felix, F.; Fergusson, J.; Gudel, H. U.; Ludi, A. *J. Am. Chem. Soc.* **1979**, *102*, 4096, 4102. (b) Kober, E. M.; Meyer, T. J. *Inorg. Chem.* **1982**, *21*, 3967. (c) Fergusson, J.; Herren, F. *Chem. Phys.* **1983**, *76*, 49.
(35) (a) Hosoya, S. *Acta Crystallogr.* **1963**, *16*, 310. (b) Lhoste, T. M.; Haug, A.; Ptak, M. *J. Chem. Phys.* **1966**, *44*, 648.
(36) (a) Calef, D. F.; Wolynes, P. G. *J. Phys. Chem.* **1983**, *87*, 3387. (b) Gennett, T.; Milner, D. F.; Weaver, M. J. *J. Phys. Chem.* **1985**, *89*, 2787. (c) Hupp, J. T.; Weaver, M. J. *J. Phys. Chem.* **1985**, *89*, 2795.

suggests that important roles are played by the relative orientation or distance of separation of the electron-transfer donor and acceptor in the electron-transfer act.

Acknowledgments are made to the National Science Foundation under Grant No. CHE-8503092 for support of this research.

Registry No. py-PTZ, 97170-93-9; PTZ, 92-84-2; 4-$ClCH_2$py, 10445-91-7; *fac*-[(bpy)Re$(CO)_3$(py-PTZ)](PF_6), 106818-73-9; (bpy)Re$(CO)_3$(TFMS), 97170-94-0; [$(bpy)_2$RuCl(py-PTZ)](PF_6), 106735-80-2; $(bpy)_2RuCl_2$, 19542-80-4; [$(bpy)_2$Ru(CH_3CN)(py-PTZ)]$(PF_6)_2$, 106735-82-4; $(bpy)_2Ru(CO_3)$, 59460-48-9; *fac*-[(bpy)Re$(CO)_3$(4-Etpy)](PF_6), 84028-69-3; [(bpy)Re$(CO)_3$(py-PTZ$^{\bullet+}$)]$^{2+}$, 106735-83-5.

Contribution from the Chemistry Department,
The University of North Carolina, Chapel Hill, North Carolina 27514

Hydrogen Atom Transfer in the Oxidation of Hydrogen Peroxide by $[(bpy)_2(py)Ru^{IV}{=}O]^{2+}$ and by $[(bpy)_2(py)Ru^{III}{-}OH]^{2+}$

John Gilbert, Lee Roecker, and Thomas J. Meyer*

Received June 25, 1986

The oxidations of H_2O_2 and of HO_2^- by $[(bpy)_2(py)Ru^{IV}(O)]^{2+}$ and $[(bpy)_2(py)Ru^{III}(OH)]^{2+}$ have been studied in aqueous solution. Rate constants and activation parameters for the oxidation of H_2O_2 by $Ru^{IV}{=}O^{2+}$ are $k(25\ °C) = 1.74 \pm 0.18$, $\Delta H^{\ddagger} = 6.0 \pm 0.3$ kcal/mol, and $\Delta S^{\ddagger} = -37 \pm 3$ eu and by $Ru^{III}{-}OH^{2+}$ are $k(25\ °C) = (8.09 \pm 0.27) \times 10^{-2}$, $\Delta H^{\ddagger} = 12 \pm 2$ kcal/mol, and $\Delta S^{\ddagger} = -38 \pm 3$ eu. H_2O/D_2O kinetic isotope ratios are, for $Ru^{IV}{=}O^{2+}$, $(k_{H_2O}{}^{25°C}/k_{D_2O}{}^{25°C}) = 22.0 \pm 1.2$ and, for $Ru^{III}{-}OH^{2+}$, $(k_{H_2O}{}^{25°C}/k_{D_2O}{}^{25°C}) = 16.2 \pm 0.7$. From rapid-mixing experiments $[(bpy)_2(py)Ru^{III}(OH)]^+$ is the initial product of the oxidation of H_2O_2 by $Ru^{IV}{=}O^{2+}$ rather than $[(bpy)_2(py)Ru^{II}(OH_2)]^{2+}$, and it is proposed that oxidation of H_2O_2 by both $Ru^{IV}{=}O^{2+}$ and $Ru^{III}{-}OH^{2+}$ occurs by H atom (1e–1 H^+) transfer.

We report here the results of a kinetic and mechanistic investigation on the oxidation of hydrogen peroxide by the Ru(IV)–oxo complex *cis*-$[(bpy)_2(py)Ru(O)]^{2+}$. The basis for our interest in the reaction are as follows. (1) It has recently been discovered that related complexes oxidize water to oxygen, and since free or bound peroxide are possible intermediates, it was of value to discover the details of how H_2O_2 is oxidized further to O_2.[1] (2) For certain $Ru^{IV}{=}O^{2+}$-based organic oxidations, it has been proposed that the redox step involves a hydride transfer.[2-4] It would be invaluable to identify such a pathway

$$Ru^{IV}{=}O^{2+} + H_2O_2 \rightarrow Ru^{II}{-}OH^+ + O_2 + H^+$$

$$Ru{-}OH^+ + H^+ \rightarrow RuOH_2^{2+}$$

or pathways

$$Ru^{IV}{=}O^{2+} + H_2O_2 \rightarrow Ru^{II}{-}OH_2^{2+} + O_2$$

in the oxidation of hydrogen peroxide. From the principle of microscopic reversibility the implications would be even more significant for O_2 reduction since it would suggest the possible existence of a concerted two-electron pathway in the reduction of O_2 to H_2O_2.

The iron porphyrin based enzymes catalase and peroxidase remove hydrogen peroxide from biological systems via two distinct mechanisms.[5] Catalase causes the decomposition of H_2O_2 by disproportionation into H_2O and O_2.[6] Peroxidase not only removes hydrogen peroxide but also takes advantage of its oxidizing equivalents to perform a variety of in vivo oxidations. The connection between these enzymes and $Ru^{IV}{=}O^{2+}$ may not be totally unreasonable in that a ferryl ($Fe^{IV}{=}O$) porphyrin group has been invoked as the active site in the enzymes.[7]

Although kinetic studies on reactions of inorganic compounds with hydrogen peroxide are numerous, many of them have focused either on complexes that contain coordination sites available for substitution by H_2O_2 (a step that can be rapid with respect to oxidation of H_2O_2) or on complexes that act strictly as outer-sphere oxidants.[8-17] The reaction of $[(bpy)_2(py)Ru(O)]^{2+}$ with hydrogen peroxide is particularly intriguing given the absence of a vacant or labile coordination site at the metal and the existence of several possible pathways for the mechanism that are more complex than simple outer-sphere electron transfer. As discussed elsewhere,[18] mechanistic evidence is available to suggest that oxo complexes of ruthenium are capable of acting as O atom donors or H atom or hydride acceptors, and all of these pathways are possibilities for the oxidation of H_2O_2. Part of this work has appeared as a preliminary communication.[19]

Experimental Section

Materials. House-distilled water was purified by distillation from alkaline permanganate. Reagent grade H_2O_2 (3%) was standardized by using $KMnO_4$ and primary standard grade As_2O_3.[20] More concentrated

(1) (a) Gersten, S. W.; Samuels, G. J.; Meyer, T. J. *J. Am. Chem. Soc.* **1982**, *104*, 4029. (b) Gilbert, J. A.; Eggleston, D. S.; Murphy, W. R., Jr.; Geselowitz, D. A.; Gersten, S. W.; Hodgson, D. J.; Meyer, T. J. *J. Am. Chem. Soc.* **1985**, *107*, 3855. (c) Honda, K.; Frank, A. J. *J. Chem. Soc., Chem. Commun.* **1984**, 635.
(2) Thompson, M. S.; Meyer, T. J. *J. Am. Chem. Soc.* **1982**, *104*, 5070.
(3) Thompson, M. S.; Meyer, T. J. *J. Am. Chem. Soc.* **1982**, *104*, 4106.
(4) Roecker, L.; Meyer, T. J. *J. Am. Chem. Soc.* **1986**, *108*, 4066.
(5) (a) Hewson, W. D.; Hager, L. P. In *The Porphyrins*; Dolphin, D., Ed.; Academic: New York, 1979; Vol. 7, p 295. (b) Duford, H. B.; Stillman, J. S. *Coord. Chem. Rev.* **1976**, *19*, 187.
(6) Hanson, L. K.; Chang, C. K.; Davis, M. S.; Fajer, J. *J. Am. Chem. Soc.* **1981**, *103*, 663.
(7) Dolphin, D. *Isr. J. Chem.* **1981**, *21*, 67.
(8) Galbacs, S. M.; Nagy, L.; Csanyi, L. J. *Polyhedron* **1982**, *1*, 175.
(9) Nagy, L.; Galbacs, Z. M.; Csanyi, L. J.; Horvath, L. *J. Chem. Soc., Dalton Trans.* **1982**, 859.
(10) Banas, B.; Mrozinski, J. *Proc. Conf. Coord. Chem.* **1980**, *8*, 11.
(11) Kozlov, Y. N.; Purmal, A. P.; Uskov, A. M. *Russ. J. Phys. Chem. (Engl. Transl.)* **1980**, *54*, 992.
(12) Sigel, H.; Flierl, C.; Griesser, R. *J. Am. Chem. Soc.* **1969**, *91*, 1061.
(13) Jarnigan, R. C.; Wang, J. H. *J. Am. Chem. Soc.* **1958**, *80*, 786.
(14) Held, A. M.; Halko, D. J.; Hurst, J. K. *J. Am. Chem. Soc.* **1978**, *100*, 5432.
(15) Heyward, M. P.; Wells, C. F. *J. Chem. Soc., Dalton Trans.* **1981**, 1863.
(16) Wells, C. F.; Fox, D. *J. Chem. Soc., Dalton Trans.* **1977**, 1498.
(17) Wells, C. F.; Husain, M. *J. Chem. Soc. A* **1970**, 1013.
(18) Meyer, T. J. *J. Electrochem. Soc.* **1984**, *131*, 221C.
(19) Gilbert, J. A.; Gersten, S. W.; Meyer, T. J. *J. Am. Chem. Soc.* **1982**, *104*, 6872.
(20) Vogel, A. I. *A. Textbook of Quantitative Inorganic Analysis*; Wiley: New York, 1961; p 295.

0020-1669/87/1326-1126$01.50/0